Biochimica et Biophysica Acta 1827 (2013) 1191–1199

Contents lists available at ScienceDirect

Biochimica et Biophysica Acta

journal homepage: www.elsevier.com/locate/bbabio

Mutational control of bioenergetics of bacterial reaction center probed by delayed fluorescence

Delphine Onidas [a,c,1], Gábor Sipka [b,1], Emese Asztalos [b], Péter Maróti [b,*]

[a] Laboratoire de Chimie Physique UMR 8000, Batiment 350, Orsay-Cedex, Université de Paris-Sud, 91405, France
[b] Department of Medical Physics, University of Szeged, Rerrich Béla tér 1, Szeged H-6720, Hungary
[c] UFR Biomédicale, Université Paris Descartes, 45 rue des Saints-Pères, F-75006 Paris, France

ARTICLE INFO

Article history:
Received 9 January 2013
Received in revised form 1 May 2013
Accepted 9 May 2013
Available online 15 May 2013

Keywords:
Bacterial photosynthesis
Reaction center protein
H-bond network
Light-induced free energy changes
Charge recombination

ABSTRACT

The free energy gap between the metastable charge separated state $P^+Q_A^-$ and the excited bacteriochlorophyll dimer P* was measured by delayed fluorescence of the dimer in mutant reaction center proteins of the photosynthetic bacterium *Rhodobacter sphaeroides*. The mutations were engineered both at the donor (L131L, M160L, M197F and M202H) and acceptor (M265I and M234E) sides. While the donor side mutations changed systematically the number of H-bonds to P, the acceptor side mutations modified the energetics of Q_A by altering the van-der-Waals and electronic interactions (M265IT) and H-bond network to the acidic cluster around Q_B (M234EH, M234EL, M234EA and M234ER). All mutants decreased the free energy gap of the wild type RC (~890 meV), i.e. destabilized the $P^+Q_A^-$ charge pair by 60–110 meV at pH 8. Multiple modifications in the hydrogen bonding pattern to P resulted in systematic changes of the free energy gap. The destabilization showed no pH-dependence (M234 mutants) or slight increase (WT, donor-side mutants and M265IT above pH 8) with average slope of 10–15 meV/pH unit over the 6–10.5 pH range. In wild type and donor-side mutants, the free energy change of the charge separation consisted of mainly enthalpic term but the acceptor side mutants showed increased entropic (even above that of enthalpic) contributions. This could include softening the structure of the iron ligand (M234EH) and the Q_A binding pocket (M265IT) and/or increase of the multiplicity of the electron transfer of charge separation in the acceptor side upon mutation.

1. Introduction

The dynamics of proteins are controlled by the complex interactions of the amino acids [1–3]. Mutations directed to key sites can cause major changes in functions and energetics of the protein [4,5]. The general principle of mutation control of redox proteins can be tested in the reaction center (RC) of photosynthetic bacteria that can serve as a model system for these studies (Fig. 1). The RC is one of few membrane proteins whose 3D structures have been obtained at higher and higher (2.5 Å [6] and 1.87 Å [7]) resolutions. The structure reveals the binding sites and precise orientation of cofactors and their interaction with proteins and provides a solid basis to interpret results of absorption and fluorescence studies at an atomic level [8]. The biochemical modification and the genetic transformation of *Rhodobacter* (*Rba.*) *sphaeroides* are well elaborated [9,10]. Additionally, the kinetics and thermodynamics of the charge transfer processes are quite easy to study by detection of flash induced absorbance changes of the cofactors in their different redox states. All these advantages allow subtle analysis of structure–energetics–function relationships including protein and electrostatic controls of the electron and proton transfer processes [11–13]. The bacterial RC performs its function with a very high quantum efficiency of near 100% [14] and has therefore long been a model protein for the study of the conversion of light into chemical energy, with relevance to the design of artificial systems [15]. Results obtained on RCs are frequently used as a basis to understand the function of similar redox and/or proton transport proteins involved in photoactive or respiratory systems [16]. Here, we aim to obtain a better understanding of which facts make the bacterial RC robust and yet flexible enough to function efficiently under different conditions.

The RC protein of purple photosynthetic bacterium *Rba. sphaeroides* binds ubiquinone (UQ) and reduced cytochrome (cyt c^{2+}) at the cytoplasmic and periplasmic sites, respectively, and releases UQH_2 and cyt c^{3+} as redox products [12,13,17,18]. The absorption of a photon results in intraprotein electron transfer from the primary electron donor (bacteriochlorophyll dimer, P, situated on the periplasmic side of the membrane) through a series of intermediates (bacteriochlorophyll monomer,

Abbreviations: BChl, monomeric bacteriochlorophyll; BPhe, bacteriopheophytin; DL, delayed light; LDAO, N,N′-dimethyldodecylamine N-oxide; P, primary electron donor, a non-covalently linked bacteriochlorophyll dimer; Q_A and Q_B, primary and secondary quinones; Rba, *Rhodobacter*; RC, reaction center; Triton X-100, octylphenol polyethylene glycol ether; UQ, ubiquinone; WT, wild type

* Corresponding author. Tel.: +36 63 544 120.
E-mail address: pmaroti@sol.cc.u-szeged.hu (P. Maróti).
URL: http://www.szote.u-szeged.hu/dmi (P. Maróti).

[1] These authors contributed equally to the present work.

0005-2728/$ – see front matter © 2013 Elsevier B.V. All rights reserved.
http://dx.doi.org/10.1016/j.bbabio.2013.05.002

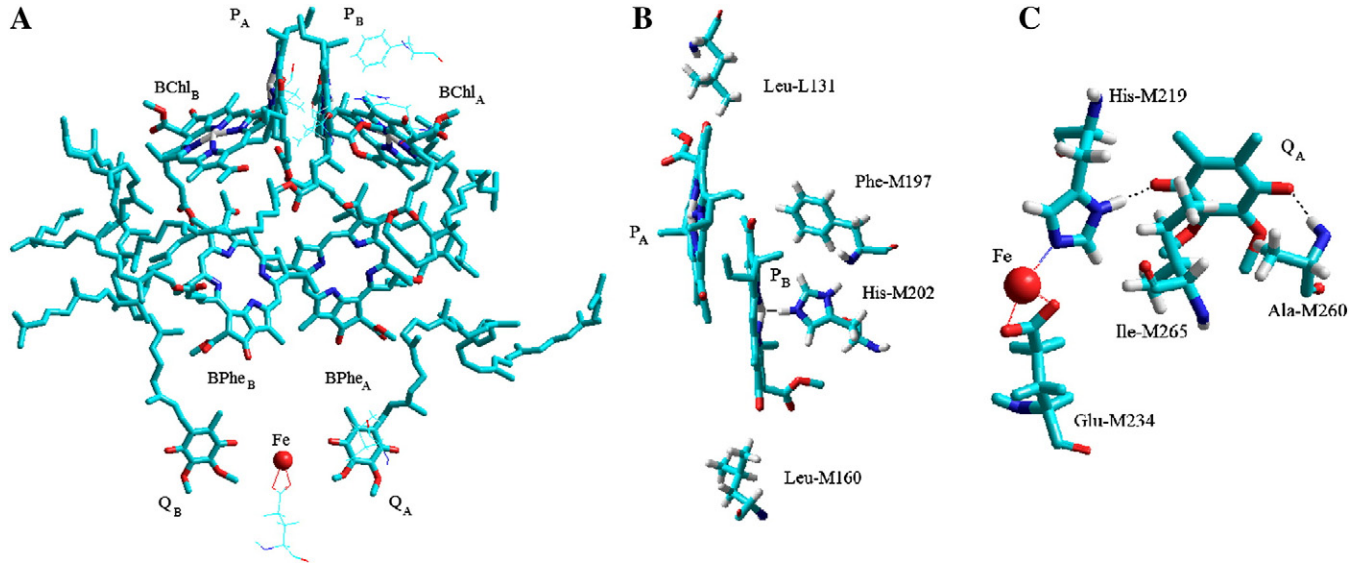

Fig. 1. The twofold symmetric arrangement of the cofactors and location of the amino acid residues targeted for mutations in the atomic structure of the wild type RC protein (Brookhaven Data Bank structure 3I4D.pdb). The periplasmic (electron donor) side is separated from the cytoplasmic (electron acceptor) side by a wide hydrophobic (membrane) band in the middle (A). The mutations directed to the indicated amino acids of the donor (B) and acceptor (C) sites cause significant alteration of the redox midpoint potentials of the dimer (P/P^+) and the primary quinone acceptor (Q_A/Q_A^-), respectively. The hydrogen bonds are shown by thin lines.

BChl and bacteriopheophytin, BPhe, in the membrane) to stable electron acceptors (ubiquinones, Q_A and Q_B on the cytoplasmic side). The cofactors are arranged along two branches (A and B) of nearly perfect mirror-symmetry, but the electron transfer in wild type RC occurs on the A branch only (Fig. 1A). A non-heme iron atom (Fe) with its ligands is situated symmetrically to both quinones and facilitates the interquinone electron transfer. After subsequent transfer of the second electron and uptake of two protons from the aqueous bulk phase, the secondary quinone is completely reduced to quinol (Q_BH_2) and leaves the RC. Thus, the light energy is converted to the reducing power of the Q_B/Q_BH_2 redox couple that can be directly used to cover the free energy need of essential biological processes (ion transport, ATP synthesis etc.) [19].

The photochemical utilization of the absorbed light energy is controlled by the free energy state of the primary stable charge pair $P^+Q_A^-$ (Fig. 2). The larger the gap between P* (the excited dimer) and $P^+Q_A^-$, the smaller the free energy that is utilized from the absorbed photon, although the stabilization of the charge pair is increased. A convenient way of determining the free energy gap is based on the measurement of delayed fluorescence from the bacteriochlorophyll dimer [20–22]. By comparison of the prompt (PF) and delayed fluorescence (DL) intensities emitted by the excited dimer, the free energy gap between P* and the charge separated state $P^+Q_A^-$ can be determined from the Boltzmann distribution of the population between the two states, so long as the DL has a negligible effect on the kinetics (total decay) of the charge pair (the DL is of "leakage" type [23]). The use of DL has the unique advantage of absolute determination of the free energy gap which goal can be rarely set for other methods. It has been applied to several related problems of the energetics of bacterial RCs including substoichiometric amounts of proton uptake by isolated RC upon Q_A reduction [24,25] or pH-independent midpoint potential of Q_A in chromatophores [26].

In this study, the question of how the free energy level of the charge separation would be modified upon mutations of some key residues on both the donor and acceptor sides of the RC is asked. The amino acids targeted for site-directed mutagenesis are demonstrated in Fig. 1A. The energetics of the donor side was changed either by modification of the hydrogen-bonding pattern of P (reviewed in [10]) or by altering the pigments forming the dimer [27] (Fig. 1B). Systematic alteration of the oxidation potential of the dimer was observed upon changing the number of hydrogen bonds between the RC subunits and the conjugated system of P by electrochemical [10,28], FTIR [29] and ENDOR [30] studies. Here, single (L131LH), double (L131LH–M160LH) and triple (L131LH–M160LH–M197FH) mutants were constructed. The change of the axial histidine ligand of P_B (M202H) to Leu resulted in a BChl–BPhe heterodimer of increased P/P^+ midpoint potential compared to WT [31]. In this study, a double mutant (M202HL + L131LH) was designed that combined the heterodimer mutation with a hydrogen-bond mutation. DL investigations have not been carried out in these mutants and new aspects of the H-bond system in homo- and heterodimer can be revealed. Similarly, information about the cytoplasmic H-bond network can be expected from mutations in the close vicinity of Q_A (M265I

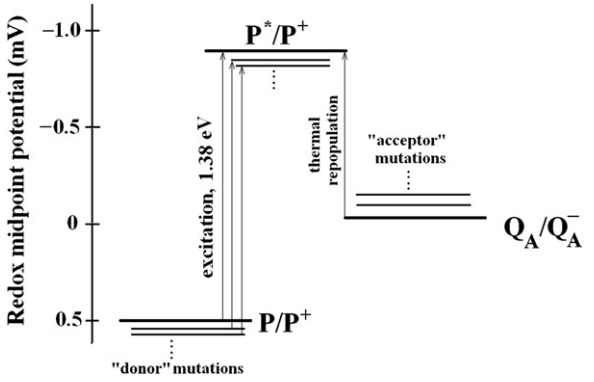

Fig. 2. Redox midpoint potentials of the cofactors playing a crucial role in generation of DL. Following the absorption of a photon of energy 1.38 eV (corresponding to 865 nm wavelength), the primary electron donor, P, a dimer of bacteriochlorophylls becomes a strong reducer in its singlet excited state P* (midpoint redox potential E'_m (P^*/P^+) ~ −900 mV). The excitation energy of P → P* remains unchanged in the donor- and acceptor side mutations used in this study. The excitation of the dimer is followed by electron transfer from P* to the primary quinone yielding the charge separated $P^+Q_A^-$ state. The approximate redox midpoints of P/P^+ and Q_A/Q_A^- of wild type RC at pH 8 are taken +500 mV and −50 mV, respectively [24]. The precursor of the DL is P* repopulated thermally from the $P^+Q_A^-$ state. Any energetic changes on the donor and acceptor sides due to mutations and/or other changes (e.g. pH) will affect the DL.

[32–34]) and the non-heme iron (M234E [35]) which alter the reduction potential of the primary quinone (Fig. 1C). As the intensity of the observed DL depends on the free energy levels of the redox cofactors P/P^+ and Q_A/Q_A^- on the donor and acceptor sides, respectively, their changes upon mutations can be nicely followed and interpreted by measurement of the DL from the bacteriochlorophyll dimer. The selected mutants show overall energetic changes that can be summed up from individual free energy changes induced by steric restrictions, electrostatics and modification of the number of H-bonds around the dimer, the primary quinone and the non heme iron atom. The thermodynamic parameters of the $P^* \rightarrow P^+Q_A^-$ process indicate an enhanced entropic term in the free energy change of the mutants at the acceptor side that shed some light on the possibility of increased structural flexibility in mutants targeting M265 and M234.

2. Materials and methods

The wild type strain and all expression strains used in this study are derived from the pink and carotenoid-containing strain 2.4.1 of *Rba. sphaeroides* cultivated under semi-aerobic conditions [36]. The construction of mutant strains harboring the different mutations, the mutagenesis procedures, growth conditions for mutant cells, as well as the RC preparation, have been described previously [37]. The cells were grown in Erlenmeyer flasks filled to 50% of the total volume with malate yeast medium supplemented with kanamycin (20 μg/ml) and tetracycline (2 μg/ml). The cultures were grown in the darkness at 30 °C on a gyratory shaker (140 rpm). The RCs were solubilized from the membrane by ionic detergent LDAO that was removed and replaced by a nonionic detergent Triton X-100 after a long (48 h) dialysis at 4 °C by a frequent change of the dialyzing medium. The pH was measured with a combined glass electrode (model 91–03; Orion) calibrated with standards that spanned the measured pH range. The assay solution contained 2 μM RCs with 0.03% Triton X-100, 100 mM NaCl, and 5 mM buffer, depending on the pH. The following buffers were used: 2-(N-morpholino)-ethanesulfonic acid (MES; Sigma) between pH 5.5 and pH 6.5; 1,3-bis[tris(hydroxymethyl) methylamino] propane (Bis–Tris propane; Sigma) between pH 6.3 and pH 9.5; Tris–HCl (Sigma) between pH 7.5 and pH 9.0; and 3-(cyclohexylamino) propanesulfonic acid (CAPS; Calbiochem) and 2-(cyclohexylamino) ethanesulfonic acid (Ches, Sigma) above pH 9.5.

The photochemical function of RC of each mutant was characterized by the near-infrared absorbance spectrum and by measurement of the flash-induced P/P^+ signal amplitude and $P^+Q_A^- \rightarrow PQ_A$ charge recombination kinetics at 860 nm. The absorbance spectroscopy was performed on a kinetic spectrophotometer of local design [24]. The secondary quinone activity of the RC was inhibited by addition of 100 μM terbutryn. The charge recombination to the ground state may occur via direct and indirect (thermally accessed through P^+BPhe^-) tunneling pathways. The observed rate constant is

$$k_{obs} = k_A + k_{BPhe} \cdot \exp(-\Delta G_{BPhe-A}/k_B T) \quad (1)$$

where k_A and k_{BPhe} represent the rate constants of the $P^+Q_A^- \rightarrow PQ_A$ and $P^+BPhe^- \rightarrow PBPhe$ charge recombinations, respectively. The rate constant k_{BPhe} is taken here to be $2 \cdot 10^7\ s^{-1}$, independent of the nature of mutations [38]. $\Delta G_{BPhe\text{-}A}$ is the free energy difference between one of the relaxed states of P^+BPhe^- and $P^+Q_A^-$ and k_BT is the Boltzmann term. For WT RC, $\Delta G_{BPhe\text{-}A} \approx 470$ meV and the direct pathway is dominant if $\Delta G_{BPhe\text{-}A} > 390$ meV [38,39] or the free energy difference (ΔG_{P^*A}) between the states P^* and $P^+Q_A^-$ is greater than 800 meV.

Delayed fluorescence measurements were performed as described in [22,26]. The home-built kinetic fluorometer was equipped with a frequency-doubled and Q-switched Nd:YAG laser (Quantel YG 781-10, wavelength 532 nm, energy 20 mJ, duration 5 ns) and the detector was protected by an electronically controlled mechanical shutter (Uniblitz VS25). The free energy drop from P^* to $P^+Q_A^-$, ΔG_{P^*A}, was calculated by comparison of the delayed and prompt fluorescence yields, according to Arata and Parson [20]:

$$\Delta G^0_{P^*A} = k_B T \cdot \ln\left(\frac{\int F_d dt}{\int F_p dt} \cdot \frac{k_d}{k_{fl}} \cdot \frac{\eta_{fl}}{\eta_{ph}}\right). \quad (2)$$

$\int F_d(t)dt$ and $\int F_p(t)dt$ are the integrated intensities of delayed and prompt fluorescence, measured in the same sample but at very different excitation intensities (both in the linear region) to give similar emission intensities. $\int F_d(t)dt$ is determined by a one-exponential fit to the decay of the delayed fluorescence signal; $\int F_p(t)dt$ is determined by electronic integration of the prompt fluorescence, using a time constant (0.1 s) similar to that of the delayed fluorescence decay time. Highly purified RC with negligible fluorescence from impurities is needed. The Boltzmann factor is k_BT (25 meV at room temperature), k_{fl} is the radiative rate constant of prompt fluorescence ($8 \cdot 10^7\ s^{-1}$, [20,21]), k_d is the rate of decay of the delayed fluorescence, η_{ph} is the quantum yield of photochemical trapping ($\approx$1.0, [14]), and η_{fl} is the quantum yield of the prompt fluorescence ($4 \cdot 10^{-4}$, [40,41]). As the $P^+Q_A^- \rightarrow PQ_A$ charge recombination kinetics are not strictly exponential [42], the determination of k_d based on single exponential decomposition of the delayed fluorescence decay may introduce some systematic errors in the determination of the free energy gap ΔG_{P^*A} [26,43].

3. Results

The kinetics of delayed fluorescence of the dimer was measured in a series of mutants at the donor (Fig. 3) and acceptor (Fig. 4) sides of the RC. In all selected mutants, both the amplitude (area) and the rate of the decay increased compared to those of the wild type.

3.1. Addition and removal of a single H-bond to the dimer

One of the most fundamental questions is how the addition and removal of the single H-bond to the dimer will change the observed delayed fluorescence. By introduction of an H-bond with the L131LH mutation, the intensity of the DL increases significantly relative to that

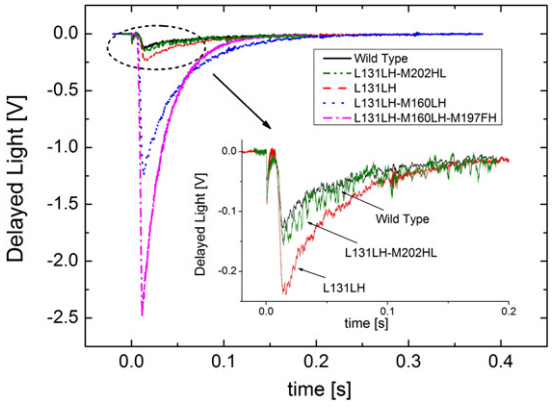

Fig. 3. Kinetic traces of the DL of donor side mutants with increasing number of H-bonds in the vicinity of the dimer. The DL increases in single (L131LH), double (L131LH–M160LH) and triple (L131LH–M160LH–M197FH) mutants relative to that of wild type RC. The introduction of histidine residue at the donor side reflects addition of one H-bond to the network around the dimer. The addition (L131LH) and subsequent removal (L131LH–M202HL) of histidine residue recover the original level of DL of the wild type RC (inset). Conditions: 2 μM RC, 100 mM NaCl, 0.03% Triton X-100, 100 μM terbutryn, pH 8 and wavelength of observed fluorescence 915 ± 10 nm. The mechanical shutter is closed during the excitation (a negligible but observable fraction of the very intense prompt fluorescence is creeping through the blades and gives the small peak at the beginning) and will open ~10 ms after the flash (see the large increase of the observed light intensity). The DL is the decaying light intensity detected in the dark. The rate constant of the decay is comparable to that of the charge recombination indicating the leakage character of the DL.

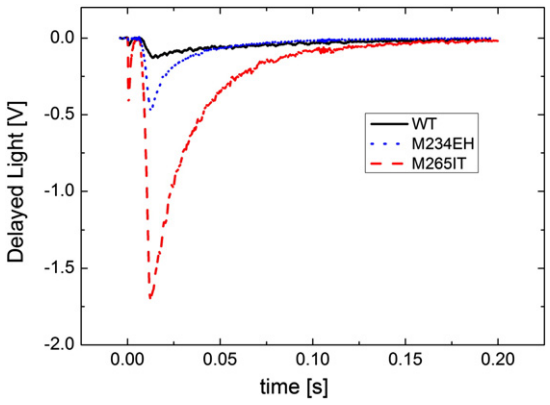

Fig. 4. Kinetic traces of the DL of acceptor side mutants in the Q_A binding pocket (M265IT) and in the iron ligand (M234EH). The conditions are the same as in Fig. 3.

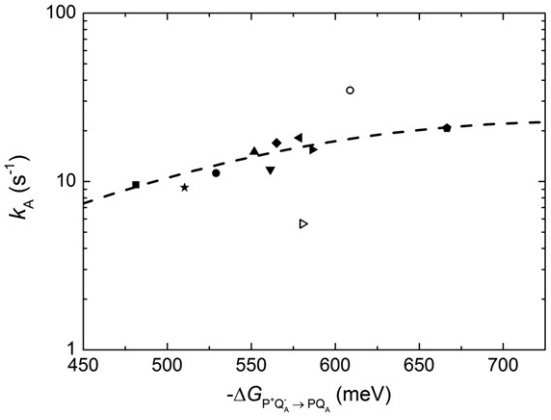

Fig. 5. The free energy dependence of the rate constants of the $P^+Q_A^- \rightarrow PQ_A$ direct charge recombination in different mutants. The rate constants were derived from the temperature-dependence of the observed rate constants according to Eq. (1). The fit to Marcus parabola (dash line) results $k_{A,\,max} = 22.6\ s^{-1}$ and $\lambda = 741$ meV for the maximum rate constant and reorganization energy of the $P^+Q_A^- \rightarrow PQ_A$ process, respectively. The data of the M265IT and L131LH–M202HL mutants are not included in the fit as they should belong to other curves of different electron transfer parameters. Notations: ■ WT, ⋆ M266HL, ● L131LH, ▲ M202HL, ▼ M234EL, ◆ M234EH, M234EA, ▷ M265IT, ► L131LH–M160LH, ○ L131LH–M202HL, and ⬟ L131LH–M160LH–M197FH.

measured in wild type RC (Fig. 3 inset). This change indicates the increase of the midpoint potential of P/P^+ due to the H-bond to the dimer in agreement with earlier electrochemical measurements [10,28]. If, however, this mutation is compensated by an additional mutation at position M202 by removal of the coordinating H-bond (M202HL), then the intensity of the DL decreases significantly close to the level of the wild type RC. The increase of the redox midpoint potential of P/P^+ attributed to the mutation L131LH is compensated by the second mutation at M202LH by lowering the midpoint potential of the dimer. In addition to these mutations, the removal of the only H-bond by L168H to the dimer in the WT yields smaller intensity of DL than that of WT. These DL experiments clearly demonstrate that the H-bond to P can be made responsible for the change of the free energy level of the dimer wherever this H-bonding to the dimeric P is occurring.

3.2. Multiple H-bond formations on the donor side

The buildup of the H-bond system around the dimer can be continued by creation of double (L131LH − M160LH) and triple (L131LH − M160LH − M197FH) mutations. In the triple mutant, the 2-acetyl and the 9-keto groups of both P_A and P_B are engaged in a hydrogen-bond with the surrounding protein (Fig. 1B). The increase of the number of H-bonds increases the intensity of the DL and the increase is stepwise: the triple mutant shows about twice as large increase as the double mutant relative to that of the wild type. The free energy levels of these H-bond mutations span about 200 meV range. Similar effect of hydrogen bonds to the conjugated carbonyls on the electrochemical titrations of these mutants was earlier observed [10,28,44]. The exact location of the new H-bond is not critical to the increase of the DL. All H-bonds to C═O groups conjugated to the chlorine rings cause changes of energetics of the dimer and the modification of the H-bond pattern around P induces similar energetic effects wherever the perturbation occurs.

3.3. The rate constants of the decay of DL as a function of free energy changes

Fig. 5 demonstrates the rate constants of the $P^+Q_A^- \rightarrow PQ_A$ direct charge recombination as a function of the driving force determined from DL measurements for several mutants. The rate constants of back reactions of the donor side mutations do not show temperature dependence (data not shown), and the charge recombination remains direct as it is in the WT. Although significant increase of the DL (decrease of ΔG_{P^*A}) is experienced, the donor side mutations do not affect $\Delta G_{BPhe\text{-}A}$ (see Fig. 2). For the acceptor side mutations at M234E and M265I, however, $\Delta G_{BPhe\text{-}A}$ gets smaller, therefore it should be considered that a significant fraction of the back reaction may occur via the indirect pathway. Indeed, the observed rate constant of the charge recombination of the M265IT mutant shows steep temperature-dependence: k_{obs} increases from 30 s^{-1} at 5 °C to 90 s^{-1} at 33 °C (data not shown). In these mutants, the rate constant of the direct recombination (k_A) is determined from k_{obs} via their different temperature-dependence (see Eq. (1)) and these values are plotted in Fig. 5.

With the exception of M265IT and M202HL + L131LH, the data obtained from very different mutations on the acceptor and donor sides line up to a single (Marcus) parabola with maximum rate constant of $k_{max} = 22.6\ s^{-1}$ and reorganization energy of $\lambda = 741$ meV [45]. As the rate constants of direct back reaction of the different mutants do not show large changes upon increase of the driving force, the reorganization energy should be close to the actual free energies. This λ value is somewhat lower than the relevant reorganization energies (800–900 meV) published earlier [10]. The recent results of electron–nuclear and electron–electron double resonance spectroscopies support this view: Q_A remains in its binding site with the same position and orientation upon reduction [46]. The quinone ring is initially in an orientation that is favorable for its light-driven reduction. This diminishes the reorganization requirements for fast electron reduction. The rate constants of the M265IT and M202HL + L131LH mutants cannot be incorporated into the Marcus parabola based on the WT RC. The discrepancy implies that these mutations cause an additional change (e.g. in reorganization energy) that influences the rate of charge recombination.

The decay rates of the DL behave very similarly to those of the charge recombination measured by absorption changes. This is in agreement with the "leakage" type of the DL in bacterial RC. For comparison, the DL or thermoluminescence from Photosystem II of green plants does not demonstrate this property, mainly due to the much smaller (ΔG_{P^*A} ~400–500 meV) free energy gap [47]. The disadvantage of much smaller DL in bacterial RC is compensated by simpler (Boltzmann) evaluation of the data.

3.4. pH-dependence of the free energy gap between P^* and $P^+Q_A^-$

The free energies of the different states can be modified not only by mutations of nearby residue(s) but by change of the pH of the medium, as well (Fig. 6). The direction of change of the free energy is explicitly related to the direction of change of pH. The proton release/binding (from energetic point of view) destabilizes/stabilizes the redox agent. The effect is small but can be measured. At low pH,

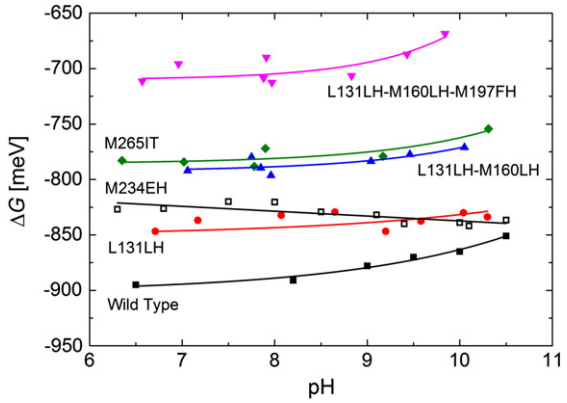

Fig. 6. The pH-dependence of the free energy drop from P* to $P^+Q_A^-$ in wild type RC and mutants at the dimer and at the Q_A binding site. ΔG_{P^*A} was determined from the intensity of delayed fluorescence, as described in the Materials and methods. Conditions: 2 μM RCs, 0.03% Triton X-100, 5 mM buffer (1 mM of each of Mes, Mops, Tricine, Ches, and Caps), 100 mM NaCl and 100 μM terbutryn.

the free energy gap is larger than at higher pH. The slope is near zero between pH 6.5 and 8.5, with some RCs showing steeper values at higher pH. Even in this range, the slopes are far away from the value of 60 meV/pH unit that directly characterizes the net uptake/release of 1 H^+ ion upon reduction/oxidation of the redox center. Neither Q_A/Q_A^- nor P/P^+ participates directly in protonation/deprotonation processes. The increased instability above pH 8 in wild type is due to acidic cluster in the vicinity of Q_B [48]. This behavior is observed in the donor side mutants and in the M256IT mutant but is completely lacking in the M234E and M266H mutants.

3.5. Thermodynamic parameters

Direct measurement of the intensity of the DL yields the free energy of the $P^+Q_A^- \rightarrow P^*$ process (ΔG_{P^*A}) that consists of enthalpic (ΔH_{P^*A}) and entropic ($T \cdot \Delta S_{P^*A}$) terms: $\Delta G_{P^*A} = \Delta H_{P^*A} - T \cdot \Delta S_{P^*A}$. As the DL originates from the leakage of the thermal equilibrium between $P^+Q_A^-$ and P*, the observation of the temperature dependence of the DL (van't Hoff plot) serves as an independent method to find the enthalpy change (ΔH_{P^*A}) of the $P^+Q_A^- \rightarrow P^*$ transition. ΔH_{P^*A} is obtained as the slope of the straight line in the van't Hoff representation (Fig. 7). From these two quantities (ΔG_{P^*A} and ΔH_{P^*A}), the third parameter, the entropy change (ΔS_{P^*A}) can be derived (Table 1).

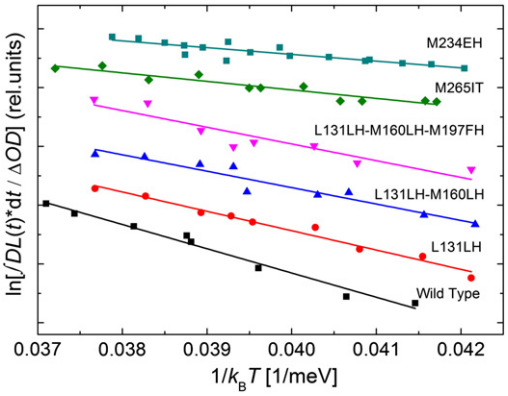

Fig. 7. van't Hoff plots of the DL in wild type and different mutants. The area of the DL traces normalized to the concentration of the RC (ΔOD is flash-induced absorption change at 430 nm) shows significant temperature-dependence: according to the Boltzmann's relationship: larger intensity of DL can be obtained at elevated temperatures. The slope corresponds to the enthalpy change of the $P^+Q_A^- \rightarrow P^*$ transition. The measured data of the different mutants are arranged (shifted) according to decreasing (increasing) slopes.

In wild type RC, the $P^+Q_A^- \rightarrow P^*$ transition is primarily driven by enthalpy change and the entropic change has not much significance [20]. The tendency is basically preserved in the donor site mutants where the enthalpic term remains dominant with slightly larger contribution of the entropic term upon increase of the number of H-bonds. The acceptor side mutations show qualitative differences: the entropy change may become a significant driving force in the $P^+Q_A^- \rightarrow P^*$ transition even after single mutation. This observation could imply molecular rearrangements in the M265IT and in the series of M234EX (where X = H, L, A and R) mutants relative to that in wild type RC. These specific and transient molecular conformations are prerequisites of the transition (charge separation/recombination) in Q_A related mutations and seem to be absent in the donor side mutations.

Within the error of the measurement, the high ionic strength of the solution (100 mM) decreases slightly the free energy gap of all mutants relative to that of low ionic strength. The enthalpy and entropy contributions are subjected to small modifications, as well. As the effect is small, it can be concluded that external charge redistributions have minor influence on the observed thermodynamic parameters.

4. Discussion

To understand the light-induced charge separation and subsequent electron transfer reactions in bacterial RC, both kinetics and thermodynamics should be measured [49]. In this study, mutants directed to specific sites on the donor and acceptor sides were constructed and the changes in energetics were followed by detection of the delayed fluorescence of the bacteriochlorophyll dimer which method has been proved to be an adequate and sensitive tool in bacterial photosynthesis to gain both kinetic and thermodynamic data. The selected mutants caused large changes of the free energies of the first metastable separated charges of P and Q_A accompanied with major modifications in their enthalpic and entropic contributions and not insignificant variations on their pH-dependence. The discussion will focus on molecular details and interpretation of these observations.

4.1. Changes of interactions in the mutants

All the mutants used in this work demonstrated large decreases in the free energy gap between P* and $P^+Q_A^-$. As none of the mutations are accompanied by major structural changes, the observed energetic changes are attributed to slight modifications of the interactions between the cofactors (P and Q_A) and the protein environment including the H-bonds to P on the periplasmic site and the extended H-bond network on the cytoplasmic site of the RC.

The effect of hydrogen bonds to the conjugated carbonyl groups on the oxidation/reduction midpoint potential of the dimer is well documented [10]. In wild type, the redox midpoint potential of P/P^+ is ~500 mV [24] and an additional hydrogen bond to the dimer raises the potential by 60 to 120 mV, while loss of the hydrogen bond decreases the potential by approximately 80 mV. The DL measurements on H-bond mutants supported these results. The free energy change caused by introduction of a single H-bond was compensated by the removal of an H-bond at a different conjugated carbonyl group of the dimer (Fig. 3) and both the rates and the amplitude (area) of the decay of DL increased with increasing number of H-bonds (Figs. 5 and 6). Although the decrease of the free energy gap determined from DL (Table 1) was not as large as those obtained from redox titration data [28], the tendency could be well recognized. The discrepancy can be attributed to the different conditions of the two measurements. While the redox equilibrium is achieved by chemical oxidation of the dimer, the DL method includes the redox changes in Q_A, as well. The interaction of the protein environment with the dimer in wild type RC sets the free energy gap the largest

Table 1
Summary of the thermodynamic parameters (changes of the free energy ($\Delta G^0_{P^*A}$), enthalpy ($\Delta H^0_{P^*A}$) and entropy ($T \cdot \Delta S^0_{P^*A}$ at room temperature)) corresponding to the $P^* \rightarrow P^+Q_A^-$ charge separation determined for wild type and mutant RCs in aqueous solutions of ionic strength 0 and 100 mM at pH 8.

	I [mM]	Mutants	$\Delta G^O_{P^*A}$ [meV]	$\Delta H^O_{P^*A}$ [meV]	$T\Delta S^O_{P^*A}$ [meV]
Wild type	0	θ	−898 ± 20	−745 ± 35	153 ± 42
	100		−890 ± 21	−765 ± 40	125 ± 47
Donor side	0	L131LH	−850 ± 22	−674 ± 24	176 ± 24
	100		−835 ± 20	−693 ± 21	142 ± 22
	0	L131LH-M160LH	−793 ± 18	−639 ± 23	154 ± 24
	100		−775 ± 21	−666 ± 38	109 ± 38
	0	L131LH-M160LH-M197FH	−713 ± 12	−342 ± 25	371 ± 25
	100		−698 ± 10	−384 ± 32	314 ± 33
	0	M202HL	−828 ± 22	−600 ± 25	228 ± 34
	100		−816 ± 21	−620 ± 35	196 ± 35
	0	M202HL-L131LH	−771 ± 18	−437 ± 36	334 ± 37
	100		−750 ± 17	−450 ± 66	300 ± 67
Acceptor side	0	M234EH	−814 ± 25	−253 ± 28	561 ± 22
	100		−801 ± 21	−243 ± 25	558 ± 25
	0	M234EL	−818 ± 27	−492 ± 67	326 ± 68
	100		−805 ± 21	−324 ± 22	481 ± 22
	0	M234EA	−801 ± 18	−426 ± 26	386 ± 26
	100		−788 ± 21	−415 ± 28	362 ± 28
	0	M234ER	−783 ± 30	−227 ± 25	556 ± 25
	100		−766 ± 21	−185 ± 26	581 ± 27
	0	M265IT	−799 ± 16	−369 ± 34	430 ± 34
	100		−784 ± 21	−316 ± 33	468 ± 34

of those studied here and assures small portion (rate) of wasteful charge recombination. The additional H-bonds in the mutations decrease the free energy gap and the yield of photochemical utilization of the absorbed photon. Systematic modulation of the H-bond pattern by mutagenesis produces a wide range of midpoint potentials of the dimer that sets the stage for building new functionality into the bacterial RC including photo-oxidation of tyrosine [50] and tight binding and oxidation of manganese [51].

The energetics of Q_A is determined by complex interactions with surrounding amino acids [18] and the mutation of M265IT used here can have several consequences. His-M219 and Ala-M260 form H-bonds with the O4 (2.87 Å) and O1 (2.82 Å) carbonyls of Q_A, respectively (structure 1AIG.pdb, Fig. 1C). Trp-M252 and Ile-M265 are on opposite sides of the quinone ring and in van der Waals contact with it. The mutations of the M265 bulky isoleucine site to smaller and polar amino acids threonine and serine led to significant redox tuning. Differences in the measured rate of charge recombination indicated that the polar mutations lowered the midpoint potential of Q_A by ~100 and 85 mV respectively [32,33]. Similar results (~105 and 60 mV for threonine and serine) were obtained when the free energy of the $P^+Q_A^-$ relative to P* was measured via the delayed fluorescence (see Fig. 4. and [43]). Several factors may result in these free energy changes but their contributions have not yet been clarified. The mutation can affect the protein–quinone interactions electrostatically or by changing the van der Waals contacts. A movement of the peptide backbone away from the quinone may increase the hydrogen bond distance between the O1 carbonyl and the Ala-M260 peptide NH by ~0.1 Å. Additionally, the difference in size (van der Waals contact) of the amino acids and the introduction of the hydroxyl group can contribute to generate the observed shift. The orientations of quinone methoxy groups that may be implicated in redox poising can play only a minor role as substituting the native ubiquinone with anthraquinone, which lacks any methoxy groups, showed similar energetic effects [33]. Recent pulsed EPR measurements provided further details but could not offer a final conclusion [34]. While nitrogen hyperfine parameters were nearly unchanged between the histidine M219 and the Q_A semiquinone, changes in the quadrupole parameters indicated a significant change in the electric field gradient. Additionally, resolution of the hyperfine coupling between the peptide nitrogen and the semiquinone decreased in the mutant. Although there is only a small effect on the binding site structure, yet it might have sufficient magnitude to suggest that the electric potential and/or field gradient are important contributions to the electronic structure and to the observed changes of the free energy.

The glutamic acid M234 develops two bonds with the Fe atom and, together with four histidines (L190His, L230His, M219His and M266His), constitutes the iron ligand (Fig. 1C). L190His and M219His are symmetrically bound to the Fe atom and also to Q_A and Q_B, with which they form H-bonds. The Q_A-M219His-Fe-L230His-Q_B "wire" has been proposed as a structural and energetic connection of the two quinone pockets [48]. Because of the central position of M234Glu, lying between the two quinones and binding the Fe atom, it may influence the

energetics of the Q_A site. Several M234EX mutants (X = H, L, A and R) with different steric and electric characteristics were included to bolster this claim. The site-specific mutant M234EH adds a fifth His to the Fe ligand and the M234EL mutant replaces a bulky non-polar amino acid that is incapable of developing interactions with the Fe atom and/or does not allow the formation of a cavity filled with water molecules. All of the mutants in this study caused severe changes in the energetics of the primary quinone detected by DL (see Table 1) and modified the H-bond network to Q_A [35].

4.2. pH-dependence of the stabilization/destabilization of the $P^+Q_A^-$ dipole

The pH-dependence of the free energy gap ΔG_{P^*A} may indicate an influence of protonation/deprotonation of the protein that accompanies the charge separation. The measured pH-dependence of the free energy change is related to the integral of the proton uptake/release induced by the $P \rightarrow P^+Q_A^-$ transition [17]. The $P^+Q_A^-$ dipole has two ends and therefore stabilization can occur by simultaneous uptake and release of protons at the quinone and dimer sides, respectively. The flash-induced uptake of 1 proton/RC by the acidic cluster near Q_B would correspond to stabilization energy of 60 meV per pH unit. The measured stabilization of the $P^+Q_A^-$ state in wild type RC (e.g. $\Delta\,\Delta G = \Delta G_{P^*A}(\text{pH } 6) - \Delta G_{P^*A}(\text{pH } 11)$) amounts to approximately 10 meV per pH unit and corresponds to substoichiometric net proton binding in agreement with earlier results [24,25].

The quinone-side mutations that modify the flash-induced uptake of H^+ ions operate in agreement with the expectations based on recent studies. It has been proposed that protons are taken up by an acidic cluster in anticooperative interaction near the Q_B. The cluster is connected to Q_A by a chain of H-bonds throughout the cytoplasmic domain of the protein [48]. The relaxation of the $P^+Q_A^-$ charge separated state and the subsequent electron transfer (charge recombination) require the spreading of the protons and the establishment of a favorable configuration for their distribution over the hydrogen bond network. This is also supported by theoretical calculations which have shown that upon formation of Q_A^-, structural waters (and associated hydrogen bond networks) on the cytoplasmic side of the RC change their orientation/occupation [52,53]. The similarity of the pH-dependence of the free energy gap between P* and $P^+Q_A^-$ of the M265IT mutant and WT is consistent with and suggestive that the extended H-bond network between Q_A and the acidic cluster is not modified. The M234EX mutants, however, have major impact on the iron ligand and the H-bond network and do not show any stabilization (rather slight destabilization) upon lowering the pH [35].

The donor side mutations in our study change the H-bond system to P and modify the stabilization of the $P^+Q_A^-$ dipole: by increase of the number of H-bonds, the destabilization will be more pronounced (Table 1). However, the change of the H-bond system to the dimer does not modify the pH-dependence of the stabilization to a significant extent, i.e. within the experimental errors (Fig. 6). Consequently, the hydrogen bonds to P do not influence the interaction between P^+ and the few protonatable surface residues made responsible for the observed small proton release from the periplasmic side upon oxidation of the dimer [17,25].

4.3. Thermodynamic parameters of the mutants

While the kinetic properties of charge separation and recombination are relatively easy to determine, the thermodynamic information is far less accessible. The thermodynamics of the charge separation reveals the difference in energy levels between the initial and final states and the driving force (Gibbs free energy) of the reaction, which is composed of enthalpic and entropic components. The partition of enthalpic and entropic contributions of the free energy change of charge separation is fraught with both real and artifactual difficulties. The results of different methodological approaches are rather obscure, conflicting and highly debated [54]. They clearly demonstrate that not all aspects of the electrostatic and conformational events accompanied with the charge separation in bacterial RC are fully understood.

Earlier calorimetric measurements showed that the charge separation did not cause significant enthalpy change, thus a large entropy decrease ($T \cdot \Delta S = -600$ meV in [55]) accounted for all of the free energy stored for the formation of $P^+Q_A^-$ from the ground state PQ_A [56,57]. The photoacoustic (PA) studies determined large enthalpic change and correspondingly null [58,59] or even positive ([60], as high as $T \cdot \Delta S = +420$ meV [61]) entropy change that was assigned to the release of the counter ions from the surface of the RC when the charge transfer canceled the dominant opposite charges. The pulsed PA measurements of formation of $P^+Q_A^-$ showed a large positive entropy not only in purple bacterial RC but in wild type Photosystem I from *Synechocystis* sp. PCC 6803 [62,63]. It was demonstrated that the A-F_X to $F_{A/B}$ step in *Synechocystis* 6803 Photosystem I was entropy driven [64]. In contrast, the $P_{680}Q_A \rightarrow P_{680}^+Q_A^-$ electron transfer in Photosystem II ($\Delta G \sim 1100$ meV) was accompanied by a small ($T \cdot \Delta S \sim 100$ meV) negative entropy change [65]. Based on PA studies on the difference in entropy between Photosystem I (and bacterial RC) and Photosystem II, it is concluded that the apparent entropy might have a vital role in photosynthetic electron transfers [63]. Additionally, it was demonstrated that entropy controlled the charge separation in artificial photosynthetic systems [66] and showed up temperature dependence of charge recombination in bacterial RC [67].

The use of the DL method to determine the entropy/enthalpy partition of free energy change upon charge separation in bacterial RC has been more limited [20,22,68] but has given less scattered results than the PA method listed above. According to DL measurements, the entropy contribution of the wild type was much less than that obtained from recent PA measurements and constituted a minor part of the free energy change (see Table 1). The apparent discrepancy may arise from a) different time regimes and b) different assumptions of the two methods. The DL method assumes equilibrium between a single charge-separated state $P^+Q_A^-$ and the excited P state on the 100 ms time scale while the PA method measures the heat released on the <100 ns time scale. The enthalpy is derived from the variation of the equilibrium constants with temperature (van't Hoff plot of the DL) or from calorimetric measurements (PA) with the assumption of temperature independent thermodynamic parameters (enthalpy, heat capacity and volume change). The latter assumption is not necessarily valid under all conditions and can cause the observed discrepancy between the two methods [67].

To explore the specific role of the protein matrix in electron transfer, the bacterial RC was genetically modified at some key amino acids and showed altered thermodynamics of electron transfer. The mutations affected the free energy change of the charge separation and increased the entropy contribution. In the triple mutant and some of the M234E mutants, it became commeasurate with the enthalpic part and in fact, the dominant term (M234EH, M234ER and M265IT). The positive sign of the entropy change upon charge separation calls attention to an increase in the number of microstates in the acceptor and/or donor sides. The small amino acid instead of the bulky isoleucine at M265 could allow for a greater number of conformations than in wild type and polar side chains from threonine could stabilize a specific and alternate methoxy conformation through H-bonding. Furthermore, the loss of H-bond between Q_A and M260A in the M265IT mutant (Fig. 1C) could increase the flexibility of the quinone ring. Similarly, the modification of the iron ligand by M234EX mutants changed the H-bond network to Q_A, and increased the number of conformations at the Q_A site relative to the WT. The observed increase of the entropy contribution in the acceptor side mutants is in agreement with softening of the H-bond structure. It is consistent with the results from neutron scattering [69], X-ray absorption fine structure spectroscopy [70] and

Mössbauer spectroscopy [71] measurements which suggested the rigidity of the native protein core around the Fe ligand that could be specifically softened by point mutations.

In addition to conformational flexibility, polar side chains and proton distribution at the cytoplasmic side of the protein might play some role in entropy increase in these mutants if they are different in the ground and charge separated states. Due to slight steric/electrostatic rearrangement caused by the mutation, some negatively charged surface groups can be reoriented (or even repelled from the RC) which is a disordering process that would enhance the entropy of the charge separation reaction. The external ionic strength of the solution had only little influence on the observed thermodynamic parameters including the entropy (Table 1). Closer knowledge of the initial and final states is required to decide which direction the change of the entropy would take.

In standard formulations of the Marcus theory, it is assumed that the vibrations coupled to electron transfer have the same frequency in reactant and product states, which implies that the entropy change is zero [45]. As small entropy change for charge separation process is measured in wild type RC, the standard formalism of the Marcus theory can be applied. For the acceptor side mutants, however, significant entropic contributions are observed and therefore the standard Marcus theory of electron transfer should be extended [63].

5. Conclusions

The delayed light emission from the dimer is one of the very few methods to measure directly the free energy change of the charge separation in bacterial RC. The selected mutants on both sides of the electron transfer revealed how the molecular interaction between the cofactors and the protein environment determines the free energy gap and how the H-bond networks extended with water molecules contribute to pH-dependent stabilization of the first non-transient dipole $P^+Q_A^-$. What we have learned here can have further perspectives in a better understanding of enzyme energetics and activity and may be relevant for designing artificial enzymes for specific activities and for drug design.

Acknowledgements

We are indebted to Dr. Pierre Sebban for his discussions at the early phase of the work and to Dr. Valérie Derrien for the preparation and cultivation of the mutants. The authors thank the CNRS–MTA bilateral agreement 2010–2011 (project n°23752), the TÁMOP 4.2.2.A-11/1KONV-2012-0060, the TÁMOP 4.2.2.B and the COST Action on "Molecular machineries for ion translocation across biomembranes" (CM0902) programs for their financial support.

References

[1] C.A. Wraight, Chance and design — proton transfer in water, channels and bioenergetic proteins, Biochim. Biophys. Acta 1757 (2006) 886–912.
[2] H. Frauenfelder, G. Chen, J. Berendzen, P.W. Fenimore, H. Jansson, B.H. McMahon, I.R. Stroe, J. Swenson, R.D. Young, A unified model of protein dynamics, P. Natl. Acad. Sci. USA 106 (13) (2009) 5129–5134.
[3] S.J. Benkovic, G.G. Hammes, S. Hammes-Schiffer, Free-energy landscape of enzyme catalysis, Biochemistry 47 (11) (2008) 3317–3321.
[4] H.E. Townley, R.B. Sessions, A.R. Clarke, T.R. Dafforn, W.T. Griffiths, Protochlorophyllide oxidoreductase: a homology model examined by site-directed mutagenesis, Proteins — Structure Function and Genetics 44 (3) (2001) 329–335.
[5] L. Wang, N.M. Goodey, S.J. Benkovic, A. Kohen, Coordinated effects of distal mutations on environmentally coupled tunneling in dihydrofolate reductase, Proc. Natl. Acad. Sci. USA 103 (43) (2006) 15753–15758.
[6] M.H.B. Stowell, T.M. McPhillips, D.C. Rees, S.M. Soltis, E. Abresch, G. Feher, Light-induced structural changes in photosynthetic reaction center: implications for mechanism of electron-proton transfer, Science 276 (1997) 812–816.
[7] J. Koepke, E.M. Krammer, A.R. Klingen, P. Sebban, G.M. Ullmann, G. Fritzsch, pH modulates the quinone position in the photosynthetic reaction center from *Rhodobacter sphaeroides* in the neutral and charge separated states, J. Mol. Biol. 371 (2007) 396–409.
[8] Z. Guo, N.W. Woodbury, J. Pan, S. Lin, Protein dielectric environment modulates the electron transfer pathway in photosynthetic reaction centers, Biophys. J. 103 (9) (2012) 1979–1988.
[9] M.R. Jones, Structural Plasticity of Reaction Centers from Purple Bacteria, in: C.N. Hunter, F. Daldal, M. Thurnauer, J.T. Beatty (Eds.), Advances in Photosynthesis and Respiration: The Purple Phototrophic Bacteria, Springer, Dordrecht, The Netherlands, 2009, pp. 295–321.
[10] J.C. Williams, J.P. Allen, Directed Modification of Reaction Centers from Purple Bacteria, in: C.N. Hunter, F. Daldal, M. Thurnauer, J.T. Beatty (Eds.), Advances in Photosynthesis and Respiration: The Purple Phototrophic Bacteria, Springer, Dordrecht, The Netherlands, 2009, pp. 337–353.
[11] P. Maróti, C.A. Wraight, Kinetics of H^+ ion binding by the $P^+Q_A^-$ state of bacterial photosynthetic reaction centers: rate limitation within the protein, Biophys. J. 73 (1997) 367–381.
[12] M.Y. Okamura, M.L. Paddock, M.S. Graige, G. Feher, Proton and electron transfer in bacterial reaction centers, Biochim. Biophys. Acta 1458 (2000) 148–163.
[13] C.A. Wraight, Proton and electron transfer in the acceptor quinone complex of photosynthetic reaction centers from *Rhodobacter sphaeroides*, Frontiers Biosci. 9 (2004) 309–337.
[14] C.A. Wraight, R.K. Clayton, The absolute quantum efficiency of bacteriochlorophyll photooxidation in reaction centers, Biochim. Biophys. Acta 333 (1973) 246–260.
[15] Chapter 55. P. Maróti, M. Trotta, Artificial photosynthetic systems. 1,694 Pages in: A. Griesbeck, et al., (Eds.), CRC Handbook of Organic Photochemistry and Photobiology, Third Edition, Vol.1, CRC Press, 2012.
[16] D. Zannoni, B. Schoepp-Cothenet, J. Hosler, in: C.N. Hunter, et al., (Eds.), Respiration and Respiratory Complexes in Advances in Photosynthesis and Respiration: The Purple Phototrophic Bacteria, Springer, Dordrecht, The Netherlands, 2009, pp. 537–561.
[17] P. Maróti, Flash-induced proton transfer in photosynthetic bacteria (minireview), Photosynth. Res. 37 (1993) 1–17.
[18] C.A. Wraight, M.R. Gunner, The Acceptor Quinones of Purple Photosynthetic Bacteria- Structure and Spectroscopy, in: C.N. Hunter, F. Daldal, M. Thurnauer, J.T. Beatty (Eds.), Advances in Photosynthesis and Respiration: The Purple Phototrophic Bacteria, Springer, Dordrecht, The Netherlands, 2009, pp. 379–405.
[19] M.R. Gunner, M. Amin, X. Zhu, J. Lu, Molecular mechanisms for generating transmembrane proton gradients, Biochim. Biophys. Acta 1827 (8-9) (2013) 892–913.
[20] H. Arata, W.W. Parson, Delayed fluorescence from *Rhodopseudomonas sphaeroides* reaction centers: enthalpy and free energy changes accompanying electron transfer from P870 to quinones, Biochim. Biophys. Acta 638 (1981) 201–209.
[21] P.H. McPherson, V. Nagarajan, W.W. Parson, M.Y. Okamura, G. Feher, pH-dependence of the free energy gap between DQ_A and $D^+Q_A^-$ determined from delayed fluorescence in reaction centers from *Rhodobacter sphaeroides* R-26, Biochim. Biophys. Acta 1019 (1990) 91–94.
[22] K. Turzó, G. Laczkó, Z. Filus, P. Maróti, Quinone-dependent delayed fluorescence from reaction centers of photosynthetic bacteria, Biophys. J. 79 (2000) 14–25.
[23] J. Lavorel, Luminescence, in Bioenergetics of Photosynthesis, Govindjee ed. Academic Press, New York, 1975. pp. 223–317.
[24] P. Maróti, C.A. Wraight, Flash-induced H^+ binding by bacterial photosynthetic reaction centers: comparison of spectrophotometric and conductimetric methods, Biochim. Biophys. Acta 934 (1988) 314–328.
[25] P.H. McPherson, M.Y. Okamura, G. Feher, Light-induced proton uptake by photosynthetic reaction centers from *Rhodobacter sphaeroides* R-26. I. Protonation of the one-electron states $D^+Q_A^-$, DQ_A^-, $D^+Q_AQ_B^-$, and $DQ_AQ_B^-$, Biochim. Biophys. Acta 934 (1988) 348–368.
[26] P. Maróti, C.A. Wraight, The redox midpoint potential of the primary quinone of reaction centers in chromatophores of *Rhodobacter sphaeroides* is pH independent, Eur. Biophys. J. 37 (2008) 1207–1217.
[27] C. Kirmaier, D. Holten, E.J. Bylina, D.C. Youvan, Electron transfer in a genetically modified bacterial reaction center containing a heterodimer, Proc. Natl. Acad. Sci. USA 85 (1988) 7562–7566.
[28] X. Lin, H.A. Murchison, V. Nagarajan, W.W. Parson, J.P. Allen, J.C. Williams, Specific alteration of the oxidation potential of the electron donor in reaction centers from *Rhodobacter sphaeroides*, Proc. Natl. Acad. Sci. U.S.A. 91 (1994) 10265–10269.
[29] E. Nabedryk, J.P. Allen, A.K.W. Taguchi, J.C. Williams, N.W. Woodbury, J. Breton, Fourier-transform infrared study of the primary electron donor in chromatophores of *Rhodobacter sphaeroides* with reaction centers genetically modified at residues M160 and residue L131, Biochemistry 32 (1993) 13879–13885.
[30] J. Rautter, F. Lendzian, C. Shulz, A. Fetsch, M. Kuhn, X. Lin, J.C. Williams, J.P. Allen, W. Lubitz, ENDOR studies of the primary donor cation radical in mutant reaction centers of *Rhodobacter sphaeroides* with altered hydrogen-bond interactions, Biochemistry 34 (1995) 8130–8143.
[31] J.P. Allen, K. Artz, X. Lin, J.C. Williams, A. Ivancich, D. Albouy, T.A. Mattioli, A. Fetsch, M. Kuhn, W. Lubitz, Effects of hydrogen bonding to a bacteriochlorophyll–bacteriopheophytin dimer in reaction centers from *Rhodobacter sphaeroides*, Biochemistry 35 (1996) 6612–6619.
[32] E. Takahashi, T.A. Wells, C.A. Wraight, Protein control of the redox potential of the primary quinone acceptor in reaction centers from *Rhodobacter sphaeroides*, Biochemistry 40 (2001) 1020–1028.
[33] T.A. Wells, E. Takahashi, C.A. Wraight, Primary quinone (Q_A) binding site of bacterial photosynthetic reaction centers: mutations at residue M265 probed by FTIR spectroscopy, Biochemistry 42 (2003) 4064–4074.
[34] E. Martin, The binding pockets of Q_A and Q_B in the photosynthetic reaction center of *Rba. sphaeroides* probed by pulsed EPR, University of Illinois, Urbana-Champaign USA, 2011. (PhD Dissertation).

[35] H. Cheap, S. Bernad, V. Derrien, L. Gerencsér, J. Tandori, P. de Oliveira, D.K. Hanson, P. Maróti, P. Sebban, M234Glu is a component of the proton sponge in the reaction center from photosynthetic bacteria, Biochim. Biophys. Acta 1787 (2009) 1505–1515.
[36] P.R. Pokkuluri, P.D. Laible, Y.L. Deng, T.N. Wong, D.K. Hanson, M. Schiffer, The structure of a mutant photosynthetic reaction center shows unexpected changes in main chain orientations and quinone position, Biochemistry 41 (2002) 5998–6007.
[37] J.A. Spitz, V. Derrien, L. Baciou, P. Sebban, Specific triazine resistance in bacterial reaction centers induced by a single mutation in the Q_A protein pocket, Biochemistry 44 (2005) 1338–1343.
[38] N.W. Woodbury, W.W. Parson, M.R. Gunner, R.C. Prince, P.L. Dutton, Radical-pair energetics and decay mechanisms in reaction centers containing anthraquinones, naphthoquinones or benzoquinones in place of ubiquinone, Biochim. Biophys. Acta 851 (1986) 6–22.
[39] P. Sebban, Activation energy of the rate constant of $P^+Q_A^-$ absorption decay in reaction centers from *Rhodobacter sphaeroides* reconstituted with different anthroquinones, FEBS Lett. 233 (1988) 331–334.
[40] K.L. Zankel, D.W. Reed, R.K. Clayton, Fluorescence and photochemical quenching in photosynthetic reaction centers, Proc. Natl. Acad. Sci. U.S.A. 61 (1968) 1243–1249.
[41] N.W. Woodbury, M. Becker, D. Middendorf, W.W. Parson, Picosecond kinetics of the initial photochemical electron-transfer reaction in bacterial photosynthetic reaction centers, Biochemistry 24 (1985) 7516–7521.
[42] B.H. McMahon, J.D. Müller, C.A. Wraight, G.U. Nienhaus, Electron transfer and protein dynamics in the photosynthetic reaction center, Biophys. J. 74 (1998) 2567–2587.
[43] L. Rinyu, E.W. Martin, E. Takahashi, P. Maróti, C.A. Wraight, Modulation of the free energy of the primary quinone acceptor (Q_A) in reaction centers from *Rhodobacter sphaeroides*: contributions from the protein and protein–lipid (cardiolipin) interactions, Biochim. Biophys. Acta 1655 (2004) 93–101.
[44] J.P. Allen, J.C. Williams, Relationship between the oxidation potential of the bacteriochlorophyll dimer and electron transfer in photosynthetic reaction centers, J. Bioenerg. Biomembr. 27 (1995) 275–283.
[45] R.A. Marcus, N. Sutin, Electron transfers in chemistry and biology, Biochim. Biophys. Acta 811 (1985) 265–322.
[46] M. Flores, A. Savitsky, M.L. Paddock, E.C. Abresch, A.A. Dubinskii, M.Y. Okamura, W. Lubitz, K. Möbius, Electron–nuclear and electron–electron double resonance spectroscopies show that the primary quinone acceptor Q_A in reaction centers from photosynthetic bacteria *Rhodobacter sphaeroides* remains in the same orientation upon light-induced reduction, J. Phys. Chem. B 114 (2010) 16894–16901.
[47] K. Cser, I. Vass, Radiative and non-radiative charge recombination pathways in Photosystem II studied by thermoluminescence and chlorophyll fluorescence in the cyanobacterium *Synechocystis* 6803, Biochim Biophys Acta 1767 (2007) 233–243.
[48] H. Cheap, J. Tandori, V. Derrien, M. Benoit, P. de Oliveira, J. Köpke, J. Lavergne, P. Maróti, P. Sebban, Evidence for delocalized anticooperative flash induced proton bindings as revealed by mutants at M266His iron ligand in bacterial reaction centers, Biochemistry 46 (2007) 4510–4521.
[49] D.N. LeBard, V. Kapko, D.V. Matyushov, Energetics and kinetics of primary charge separation in bacterial photosynthesis, J. Phys. Chem. B 112 (2008) 10322–10342.
[50] L. Kálmán, R. LoBrutto, J.P. Allen, J.C. Williams, Modified reaction centers oxidize tyrosine in reactions that mirror Photosystem II, Nature 402 (1999) 696–699.
[51] L. Kálmán, M.C. Thielges, J.C. Williams, J.P. Allen, Proton release due to manganese binding and oxidation in modified bacterial reaction centers, Biochemistry 44 (2005) 13266–13273.
[52] E. Alexov, J. Miksovska, L. Baciou, M. Schiffer, D.K. Hanson, P. Sebban, M.R. Gunner, Modeling the effects of mutations on the free energy of the first electron transfer from Q_A^- to Q_B in photosynthetic reaction centers, Biochemistry 39 (2000) 5940–5952.
[53] B. Rabenstein, G.M. Ullmann, E.W. Knapp, Electron transfer between the quinones in the photosynthetic reaction center and its coupling to conformational changes, Biochemistry 39 (2000) 10487–10496.
[54] R. Delosme, On some aspects of photosynthesis revealed by photoacoustic studies: a critical evaluation, in: J.T. Beatty Govindjee, H. Gest, J.F. Allen (Eds.), Discoveries in Photosynthesis (Advances in Photosynthesis and Respiration), Springer, 2005, pp. 651–663.
[55] H. Arata, W.W. Parson, Enthalpy and volume changes accompanying electron transfer from P-870 to quinones in *Rhodopseudomonas sphaeroides* reaction centers, Biochim. Biophys. Acta 636 (1981) 70–81.
[56] G.D. Case, W.W. Parson, Thermodynamics of the primary and secondary photochemical reactions in *Chromatium*, Biochim. Biophys. Acta 253 (1971) 187–202.
[57] J.B. Callis, W.W. Parson, M.M. Gouterman, Fast changes of enthalpy and volume on flash excitation in *Chromatium* chromatophores, Biochim. Biophys. Acta 267 (1972) 348–362.
[58] C. Nitsch, G.H. Schatz, S.E. Braslavsky, Laser-induced optoacoustic calorimetry of primary processes in cells of *Rhodospirillum rubrum*, Biochim. Biophys. Acta 975 (1989) 88–95.
[59] O.V. Puchenkov, Z. Kopf, S. Malkin, Photoacoustic diagnostics of laser-induced processes in reaction centers of *Rhodobacter sphaeroides*, Biochim. Biophys. Acta 1231 (1995) 197–212.
[60] S. Malkin, O. Canaani, The use and characteristics of the photoacoustic method in the study of photosynthesis, Annu. Rev. Plant. Physiol. Plant. Mol. Biol. 45 (1994) 493–552.
[61] G.J. Edens, M.R. Gunner, Q. Xu, D. Mauzerall, The enthalpy and entropy of reaction for formation of $P^+Q_A^-$ from excited reaction centers of *Rhodobacter sphaeroides*, J. Am. Chem. Soc. 122 (2000) 1479–1485.
[62] H.J.M. Hou, V.A. Boichenko, Y.C. Wang, P.R. Chitnis, D. Mauzerall, Thermodynamics of electron transfer in oxygenic photosynthetic reaction centers: a pulsed photoacoustic study of electron transfer in Photosystem I reveals a similarity to bacterial reaction centers in both volume change and entropy, Biochemistry 40 (2001) 7109–7116.
[63] H.J.M. Hou, Enthalpy, entropy, and volume changes of electron transfer reactions in photosynthetic proteins, in: M. Tadashi (Ed.), Application of Thermodynamics to Biological and Materials Science, InTech, ISBN: 978-953-307-980-6, 2011, pp. 93–110, Chapter 3.
[64] H.J.M. Hou, D. Mauzerall, The A-F_X to $F_{A/B}$ step in *Synechocystis* 6803 Photosystem I is entropy driven, J. Am. Chem. Soc. 128 (2006) 1580–1586.
[65] H.J.M. Hou, V.A. Boichenko, B.A. Diner, D. Mauzerall, Thermodynamics of electron transfer in oxygenic photosynthetic reaction centers: volume change, enthalpy, and entropy of electron transfer reactions in manganese-depleted Photosystem II core complexes, Biochemistry 40 (2001) 7117–7125.
[66] A.C. Rizzi, M. van Gastel, P.A. Liddell, R.E. Palacios, G.F. Moore, G. Kodis, A.L. Moore, T.A. Moore, D. Gust, S.E. Braslavsky, Entropic changes control the charge separation process in triads mimicking photosynthetic charge separation, J. Phys. Chem. A 112 (2008) 4215–4223.
[67] Q. Xu, M.R. Gunner, Temperature dependence of the free energy, enthalpy, and entropy of $P^+Q_A^-$ charge recombination in *Rhodobacter sphaeroides* R-26 reaction centers, J. Phys. Chem. B 104 (2000) 8035–8043.
[68] R.P. Carithers, W.W. Parson, Delayed fluorescence from *Rhodopseudomonas viridis* following single flashes, Biochim. Biophys. Acta 387 (1975) 194–211.
[69] S. Sacquin-Mora, P. Sebban, V. Derrien, B. Frick, R. Lavery, C. Alba-Simionesco, Probing the flexibility of the bacterial reaction center: the wild-type protein is more rigid than two site-specific mutants, Biochemistry 46 (51) (2007) 14960–14968.
[70] G. Veronesi, L. Giachini, F. Francia, A. Mallardi, G. Palazzo, F. Boscherini, G. Venturoli, The Fe^{2+} site of photosynthetic reaction centers probed by multiple scattering XAFS spectroscopy: improving structure resolution in dry matrices, Biophys. J. 95 (2) (2008) 814–822.
[71] A. Hałas, A. Orzechowka, V. Derrien, A.I. Chumakov, P. Sebban, J. Fiedor, M. Lipińska, M. Zając, T. Ślęzak, K. Strzałka, K. Matlak, J. Korecki, L. Fiedor, K. Burda, The dynamics of the non-heme iron in bacterial reaction centers from *Rhodobacter sphaeroides*, Biochim Biophys Acta 1817 (12) (2012) 2095–2102.